SEISMIC SHEAR WAVE OBSERVATIONS

IN A

PHYSICAL MODEL EXPERIMENT

Robert H. Tatham, Donald V. Goolsbee, Wulf F. Massell, Petty-Ray Geophysical and H. Roice Nelson, Seismic Acoustic Laboratory, University of Houston

This is a preprint subject to revision. Paper to be presented at the 51st Annual International Meeting of the Society of Exploration Geophysicists.

October 11 - 15, 1981

Los Angeles, California

Society of Exploration Geophysicists
Box 3098
Tulsa, Oklahoma 74101

Seismic Shear Wave Observations in a Physical Model Experiment
(Title)

by

Robert H. Tatham*, Donald V. Goolsbee*, Wulf F. Massell*, H. Roice Nelson**
(Author)

* Petty-Ray Geophysical, Geosource Inc.
** Seismic Acoustic Laboratory, University of Houston
(Company)

SEISMIC SHEAR WAVE OBSERVATIONS
IN A PHYSICAL MODEL EXPERIMENT

Robert H. Tatham*, Donald V. Goolsbee*, Wulf F. Massell*, and H. Roice Nelson**

* Petty-Ray Geophysical Division, Geosource Inc.
** Seismic Acoustic Laboratory, University of Houston

ABSTRACT

Observations of mode-converted Shear Waves (SV) were made in a physical model constructed at the Seismic Acoustic Laboratory of the University of Houston. Some aspects of the model were designed to simulate the marine observations reported for the offshore MAFLA area (Tatham and Stoffa, 1976). The model represented water depth scaled to 250 feet, the first sub-sea reflector at 4,000 feet, and the last reflector at 7,000 feet below the sea floor. Very efficient mode conversion, from P to SV and back to P, is anticipated for angles of incidence at the sea floor between 35 degrees to 80 degrees.

The model was constructed of Plexiglas and 3180 resin, materials that will support elastic shear wave propagation. One anticipated problem, internal reflections from the sides of the model, was solved by tapering the sides of the model to 45 degrees off vertical. The P-wave reflection coefficient at an interface between Plexiglas and water is 35% for vertical incidence, but diminishes to very nearly zero between 43 degrees and 75 degrees. Thus, by tapering the sides of the model, any undesired internal reflections had to undergo at least two reflections at angles of incidence in the low reflection coefficient range for P-waves. By this means, later-arriving spurious P-wave reflections were minimized.

Data were gathered in both an end-on CDP mode, with off-sets from 1,000 feet to 20,000 feet, and a variety of walk-away experiments with scaled ranges from 1,000 feet to 31,000 feet. Processing and analysis of the data confirm the existence of mode-converted shear-wave reflections in a modeled marine environment. In particular, the S-wave reflections from the 4,000 foot and 7,000 foot reflector are identified on both the 100% gathered records and the final stacked records. These SV-wave reflections were isolated for stacking by considering those portions of the gathered records, both offset and arrival time, that correspond to optimum angles of incidence. In addition, Tau-p processing isolated particular angles of incidence, further confirming the incidence angle-range criterion. Thus, the events are unambiguously identified as mode-converted shear waves.

INTRODUCTION

Recent success in developing seismic shear-wave techniques of petroleum exploration in land environments gives us encouragement to re-examine possible shear-wave sources for the marine environment. Possible methods include placing both sources and receivers on the sea floor with direct generation and recording of seismic shear waves. This represents a direct extension of land techniques and may be applicable to some shallow water areas where the sediments at the sea floor will support shear-wave propagation. For deep water, or areas with unconsolidated sediments, such direct methods may not be possible. Conventionally generated P-waves, however, are converted to shear waves (SV polarization) when interacting with a discontinuity in elastic parameters, such as the water bottom or base of unconsolidated sediments. Such a method of recording shear-wave data in a marine environment was suggested by Tatham and Stoffa (1976).

Since the publication of that paper, viable shear-wave sources for land operations operations have evolved and recent attention has been directed to evaluating the interpretational value of S-wave data. Industry interest in the potential usefulness of shear-wave recording and interpretation is reflected in the report of over 125 crew months (about 6000 miles) of land shear-wave recording during 1980 (Senti, 1981). With this expression of interest in shear-wave recording we are re-examining some of the challenging problems in developing marine shear-wave sources.

MODE-CONVERSION

In general, when P-wave energy propagating in a solid material encounters an impedance discontinuity, four outgoing seismic waves result: reflected P and S-waves and refracted P and S-waves. If the incident wave is propagating in a water layer, however, there can be no reflected S-wave. In such a case, illustrated in Figure 1, the incident P-wave impinges on the water bottom (or base of unconsolidated sediments) and energy is partitioned into three waves - reflected P, refracted P, and refracted (mode-converted) S. As i, the angle of incidence, increases mode conversion to shear-waves generally becomes more efficient. Further, as i exceeds the P-wave critical angle no P-wave energy is refracted into the sub-sea sediments. For these angles, only two possible avenues of energy propagation are available--the reflected P-wave and the refracted (mode-converted) S-wave. For some contrasts in elastic constants most of the incident energy goes into the refracted S-wave and, for other elastic parameters, most of the energy is reflected as a P-wave. For sub-sea sediments with a P-wave velocity between 6500 - 9000 ft./sec., a range that includes many shallow sedimentary rocks, the mode conversion is extremely efficient (Tatham et al, 1977).

Figure 2 illustrates the recording geometry for observing mode-converted S-waves. We assume that the ray of interest leaves the source as a P-wave, is converted from a P-wave to an S-wave (SV) at only one interface (such as the water bottom or base of unconsolidated sediments), is reflected from depth as an S-wave, and then undergoes mode-conversion from an S-wave to a P-wave upon re-entering the upper (water) layer. Keep in mind that mode-conversion occurs only for non-vertical angles of incidence. Since mode-conversion becomes more efficient as the angle of incidence increases, we would expect to observe mode-converted arrivals primarily on the longer-offset traces of multifold CDP data.

This double mode conversion may, at first thought, appear rather esoteric. It is, however, equivalent to the SKS phase of earthquake seismology, except that we also include a reflection. Richter (1958) points out (pg. 259) that the observed SKS phase, at the proper ranges, is often large and increases in amplitude with increasing range (pg. 273).

Figure 3 shows the anticipated amplitude (displacement potential) for all angles of incidence, for plane P-waves converted to S-waves at the water bottom, and with another mode-conversion back to P-wave upon re-entering the water layer. The elastic parameters used for the calculation were determined by velocity analysis of the data considered by Tatham and Stoffa (1976). The amplitude is the fraction of the incident P-wave for just the two transmission mode-conversion coefficients, ignoring attenuation and the shear-wave reflection coefficient of the subsurface reflector. Note that for angles of incidence less than the critical angle of P-waves (39°), the resulting amplitude ranges from 5 to 20 percent of the incident P-wave amplitude. Beyond the critical angle, however, the S-wave reflection with two mode-conversions has an amplitude nearly equal to the reflection coefficient of the S-wave; i.e., most of the energy is mode-converted rather than reflected at the water bottom. Recall that beyond the critical angle no P-wave energy penetrates the subsurface.

PREVIOUS INVESTIGATION

As mentioned above, the earlier work of Tatham and Stoffa (1976) made suggestions of observations of mode-converted shear-waves for some routinely recorded marine data offshore the Florida Panhandle. The observed SV waves were, at best, weak. The disparity between predicted and observed amplitudes for the shear-wave energy is attributed to the rather long (435 ft.) hydrophone groups contained in the recording array. The suppression of the low velocity events that traveled most of their travel path as SV-waves is nearly 80 percent Figure 4 shows the array response, adapted to angle of incidence, multiplied by the mode-conversion curves of Figure 3. Note that the observed events, accounting for source-array response and ignoring attenuation, should be at most 21% of that predicted by the mode-conversion curves alone. This value is in accordance with the reported observations.

In spite of these rather weak events, both P and S-wave velocity profiles were constructed and are shown in Figure 5. These interpreted velocity profiles were, to some degree, used as a basis for constructing the physical model.

PHYSICAL MODEL STUDY

The Seismic Acoustic Laboratory at the University of Houston operates a large water filled tank for gathering ultrasonic acoustic data over physical models representing earth structures. Model scaling is such that one inch on a model represents 1000 ft. of real earth, ultrasonic frequencies scale to seismic frequencies, and velocities scale to 2.4 times the velocity of the real materials. Thus, water has a model velocity of 12,000 ft./sec., and data were typically recorded at a scaled sample interval of 1 ms.

Model Construction

A physical model to test the recording of mode-converted shear-wave data was constructed at the Seismic Acoustic Lab. The materials, listed in Table 1, were chosen such that mode-converted shear-waves should be observed. The physical dimensions were sufficient to allow a single walk-away spread to a total scaled distance of over 30,000 ft. and an end-on marine cable configuration could be simulated with range up to 20,000 ft. The structure, varying only slightly with a short 9 1/2° ramp, was essentially two-dimensional. The first reflector, as shown in Figure 6, is at a scaled depth of 4,000 ft. (4" in the model) with a 1000 ft. ramp in the center of the model. The last layer is 1,000 ft. thick and the total model thickness scales to 7,000 ft. The mode-conversion coefficients for Plexiglas and water are shown in Figure 7. This compares quite favorably with the curve developed for offshore Florida. The normal incidence reflection coefficient between the Plexiglas and 3180 resin is about 3.5 percent and about 35 percent between the Plexiglas and water.

One anticipated problem was undesired P-wave energy being reflected and scattered from the sides of the model and arriving at the receiver ahead of the desired S-wave reflections. Attenuation of such spurious energy was realized by tapering the sides of the model to 45°. This design was selected to exploit low P-wave reflection coefficients in a 43-85° range, as shown in Figure 8. The P-waves are incident upon the Plexiglas - water boundary from within the Plexiglas. As illustrated in Figure 9, at least two reflections with angles of incident in the 43 - 80° range are required for any ray to return to the surface of the model. Hence, almost no spurious P-wave energy is seen in the records.

Test Data

Figure 10 shows a walk-away spread with a shot spacing of 100 ft., the near off-set of 1000 ft. and the longest off-set of 31,000 ft. The source and detector were 0.25 inches (250 scaled feet) above the solid Plexiglas interface, thus at an equivalent water depth of 250 ft. The immersion in the water, however, eliminated the usual free-surface, and thus we see no waveguide effects due to the water layer. Many reflected waves, as well as direct arrivals, are observed and will be discussed below.

In addition to the walk-away spread, a conventional end-on CDP marine line was recorded. Both shot and detector spacing was 200 ft., with ranges from 1000 to 20,000 ft. This led to a maximum CDP coverage of 48 fold, with considerable taper at the ends of the lines.

Figure 11 shows a conventional P-wave stack, utilizing ranges of 1,000 to 8,000 ft. (18 fold) in the gathers. Note the presence of the ramp at 0.4 to 0.9 seconds at the center of the model. Figure 12 shows the stack with shear-wave velocities. Ranges from 5600 ft. to 25,000 ft. were considered in the gathers, but some muting was applied to use only longer ranges at greater reflection times. Since S-wave velocities are about one-half the P-wave velocities, the S-wave section is displayed at one-half the time scale of the P-wave section, and thus the P and S-wave events should be nearly correlative. Note the presence of the ramp at 1.00 to 1.40 seconds on the S-wave section, as well as all the reflections observed on the P-wave section, thus fully confirming the presence of mode-converted shear-wave (SV) reflections.

Tau-p Processing

Applying a Tau-p transform (slant-stack) to the shot-oriented field data, or CDP gathers, will display the data as a function of angle of incidence. (See Stoffa et al., 1981, for development of the Tau-p transform.) Figure 13 represents a Tau-p transform applied to the data shown in Figure 10. Note that the reflection hyperbolae of Figure 10 is seen as ellipses in Figure 13. Also note the strong change in character at the critical angle. The ellipses beyond the critical angle are mode-converted shear waves.

An inverse transform can be applied to the data of Figure 13a, resulting in the original shot-oriented field record, or the original CDP gather. Figure 13b is the same data as 13a, but with some noise at low Tau and for low p eliminated. It is this data-set to which the inverse transforms are applied.

Figure 14 represents an inverse transform applied to all the data in Figure 13b. Comparison with Figure 10 confirms the success of this inversion. Figure 15 in an inversion, to record space, of the data in Figure 13b, but using only those ray parameters (0 to 42 X 10^{-6} sec./ft.) corresponding to angles of incidence between 0 and 33 degrees. That is, no post-critical reflections are considered. Note the improvement in the overall quality of the P-wave reflections. Figure 16 is a similar inversion of the data in Figure 13b, but with ray parameters restricted (p from 55 X 10^{-6} to 80 X 10^{-6} sec./ft.) to angles of incidence between 40 and 75 degrees. Note the presence of reflections, with curvature consistent with S-wave velocities, at the longer ranges.

Further Tau-p processing was applied to the CDP gathered records constructed from the end-on marine profile. Only those CDP gathered records with offsets of 1,000 to 20,000 ft. were considered (48 fold). A forward Tau-p transform was applied to each record and two inverse transforms were then applied. The result was two sets of CDP gathers, one with a range of ray parameters consistent with P-wave data and another consistent with S-wave data. That is, the P-wave gathers represent angles of incidence between vertical and 35 degrees while the S-wave gathers represent angles of incidence between 40 and 75 degrees.

Figure 17 is a stack of the P-wave gathers, and Figure 18 is a stack of the S-wave gathers. Comparison of the data in Figures 17 and 18 with the conventionally stacked data in Figures 11 and 12 adds confidence to the original identification of the P and S-wave reflections and shows some of the potential of Tau-p processing of seismic reflection data.

DISCUSSION AND CONCLUSIONS

The observation and CDP processing capability of mode-converted shear-waves has been demonstrated for real data collected in a physical model experiment. That is, observation of shear-wave energy in data generated and recorded as P-waves in a marine environment has been confirmed. The primary difference between the recording geometry and that employed in a typical marine setting was the large off-sets (up to 20,000 ft.) applied. Examination of the walk-away analysis suggests that shear-waves may have been successfully stacked with a maximum range as short as 16,000 ft. but this is still greater than a typical marine configuration.

A significant difference between the model and real marine case is the absence of the water layer itself in the model. Thus, no guided waves in the water - layer waveguide were present to further contaminate our observations. The scaled velocities of the model were different than for the real earth, but the consistency of velocity ratios across interfaces yields this problem insignificant.

This study suggests tht future work should be applied to actual off-shore situations. Some operational problems, such as large off-sets, can be overcome. Possible anisotropy effects, however, may be difficult to correct for. Levin (1979, 1980) suggests that rock anisotropy may have a strong effect on the SV polarized shear waves. Actual experiment will be required to fully describe this potential problem.

ACKNOWLEDGEMENTS

We wish to thank Petty-Ray Geophysical, Geosource Inc., for the encouragement to conduct these experiments and publish the results.

REFERENCES

Levin, F.K.; (1979); Seismic Velocities in Transversely Isotropic Media; Geophysics, V. 44, pp 918 - 936.

Levin, F.K.; (1980); Seismic Velocities in Transversely Isotropic Media, II; Geophysics, V. 45, pp 3 - 17.

Richter, C. F.; (1958); Elementary Seismology; W. H. Freeman and Co., San Francisco.

Senti, R.J.; (1981); Special Report, Geophysical Activity in 1980; Geophysics, V. 46, pp 1316 - 1333.

Stoffa, P.L.; Buhl, P.; Diebold, J.B.; and Friedemann, W.; (1981); Direct Mapping of Seismic Data to the Domain of Intercept Time and Ray Parameter A Plane-Wave Decomposition; Geophysics, V. 46, pp 255 - 267.

Tatham, R.H.; Danbom, S.H.; Tyce, R.C.; and Omnes, G.C.; (1977); "Seismic Parameters and their Estimation: Progress in Estimation and Interpretation, Segment VI of SEG Continuing Education School, The Stationary Convolutional Model of the Reflection Seismogram and Progress in Measurement of Subsurface Seismic Parameters: Velocity, Density, Specific Attenuation", Houston, Texas; November 28-29, 1977.

Tatham, R.H.; and Stoffa, P.L.; (1976); V_p/V_s - A Potential Hydrocarbon Indicator; Geophysics, V. 41, pp 837 - 849.

	ρ (gm/cm³)	ACTUAL VELOCITY (ft/sec)	SCALED VELOCITY (ft/sec)
WATER	1.00	5,000	12,000
PLEXIGLAS	1.17	V_P = 9,000 $V_S \approx$ 4,500	V_P = 21,600 $V_S \approx$ 10,800
3180 RESIN	1.42	V_P = 8654 $V_S \approx$ 4327	V_P = 20,770 $V_S \approx$ 10,385

TABLE 1

FIGURE CAPTIONS

Figure 1 Three outgoing seismic waves that result from an incident P-wave (in a liquid) striking a liquid-solid interface: the reflected P-wave, refracted P-wave and refracted (mode-converted) S-wave. Beyond the critical angle, there is no P-wave energy refracted into the subsurface.

Figure 2 Geometry of a typical marine seismic recording array, showing a conventionally reflected P-wave and a mode-converted PSSP ray, at large angle of incidence, being detected at large off-set.

Figure 3 Amplitude, as a fraction of the original P-wave amplitude, for a doubly mode-converted wave (PSSP) at all angles of incidence. Note large amplitude of P-wave, after two mode-conversions, at large angles of incidence (from the vertical) beyond the critical angle. The water has a P-wave velocity of 5000 ft./sec. and a density of 1.0 gm/cc. Sediments have a P-wave velocity of 7850 ft./sec., an S-wave velocity of 4036 ft./sec. and a density of 2.3 gm/cc.

Figure 4a Array response, as a function of angle of incidence, for the 435 ft. hydrophone arrays employed in recording the data reported by Tatham and Stoffa (1976). Near-surface (water) velocity was assumed to be 5000 ft./sec., and the response is plotted for 20 and 30 Hz signals.

Figure 4b Applying mode-conversion coefficients from Figure 3 to the 20 Hz array-response curve in Figure 4a. Note that the maximum anticipated amplitude, accounting for array response, is only 21% of the original P-wave amplitude.

Figure 5 P and S - wave velocity profiles, as a function of depth, for an area offshore the Florida panhandle. (After Tatham and Stoffa, 1976).

Figure 6 Cross-section of physical model constructed at the Seismic Acoustic Laboratory at the University of Houston. First layer is 4" thick, which scales to 4000 ft. (scale factor is 1" = 1000 ft.). The 1000 ft. (scaled) ramp in the center of the model adds structural interest. The distance D between source and top of model scales to 250 ft. The model is immersed in water to conduct the experiment. Physical properties of water, Plexiglas and 3180 resin are summarized in Table I.

Figure 7 Mode - conversion coefficients (amplitude) for water - Plexiglas interface. Note similarity to Figure 3.

Figure 8 Reflection coefficients (energy), as a function of angle of incidence, for a P-wave incident upon a Plexiglas-water interface. P-wave is incident upon the interface from within the Plexiglas. Note the low value of P-wave reflection coefficient for angles between 40 degrees and 70 degrees.

Figure 9 Two ray paths for a ray travelling toward a 45 degree corner in Plexiglas. Note that, for an outgoing ray to leave the corner area toward the upper surface of the model, it must have at least two reflections at angles of incidence between 40 degrees and 70 degrees.

Figure 10 Data recorded over the physical model. Ranges (off-sets) are 1000 ft. (scaled) to 31000 ft., source and detector (P-wave transducers) were 250 ft. above the solid interface, and the walk-away was done in 100 ft. steps. Note numerous reflection and refraction events.

Figure 11 Conventional P-wave CDP stack of data collected over the physical model. Ranges of 1000 ft. to 8000 ft. were used, and the 200 ft. shot spacing yields an 18 fold CDP stack. Note the reflections at the lower Plexiglas-resin interface at 0.4 sec., the resin-Plexiglas interface (including ramp) at about 0.5 sec. on the left-side of the section, and the base of the model (Plexiglass-water interface) at about 0.7 sec. No reflection is observed from the top of the model, with depth of 250 ft. and minimum hydrophone off-set of 1000 ft.

Figure 12 CDP stack of data collected over the physical model, but applying shear-wave velocities. Ranges of 5600 ft. to 25000 ft. were employed. Since S-wave velocity is about one-half the P-wave

Figure 12 (con't) velocity, the time - scale of the display is one - half that of Figure 11. Note reflections from Plexiglas - resin interface at about 0.74 sec., resin-Plexiglas interface that includes the ramp, and the base of the model (Plexiglas-water) at 1.35 sec. The observed events correlate very well with the events observed in the P-wave data. The 180 degrees phase-reserval is consistant with the double mode-conversion.

Figure 13a Tau-p transform (slant - stack) applied to data (single field record) shown in Figure 10. Vertical axis is time, and each trace represents a constant ray parameter p. Knowing the water velocity, each ray parameter represents a particular angle of incidence. Note difference in character beyond the critical angle. Reflection hyperbolae appear as ellipses in the Tau-p transform. The ellipses beyond the critical angle are shear-wave (mode-converted) reflections.

Figure 13b The Tau-p transform (slant-stack) shown in Figure 13a, but with some muting of noise applied at low p and low Tau values.

Figure 14 Inverse transform (slant - stack) applied to data in Figure 13b. Note similarity to Figure 10, but with some noise removed. The noise was muted in the Tau-p transform space.

Figure 15 Inverse transform applied to data in Figure 13b, but including only ray parameters at angles of incidence less than the critical angle. Thus, this record is primarily P-wave energy.

Figure 16 Inverse transform applied to data in Figure 13b, but including ray parameters at angles of incidence between 40 degrees and 75 degrees. Thus, this record is primarily S-wave energy and low-velocity noise. The S-wave reflections show curvature.

Figure 17 Stack of CDP gathers, at P-wave velocity, after the gathered records were transformed (slant-stack) to Tau-p space, and inverse-transformed with angles of incidence less than the critical angle. Only full 48 fold gathers were used, thus the lack of stacked traces from the CDP taper. Comparison with Figure 11 confirms the success of this procedure.

Figure 18 Stack of CDP gathers, at S-wave velocities, after the gathered records were transformed (slant-stack) to Tau-p space, and inverse-transformed with angles of incidence between 40 degrees and 75 degrees. As with the P-wave stack, only full 48 trace gathers were used, and thus the lack of stacked traces from the CDP taper. Comparison with Figure 12 further confirms that these stacked events represent mode-converted shear-waves from angles of incidence beyond the critical angle.

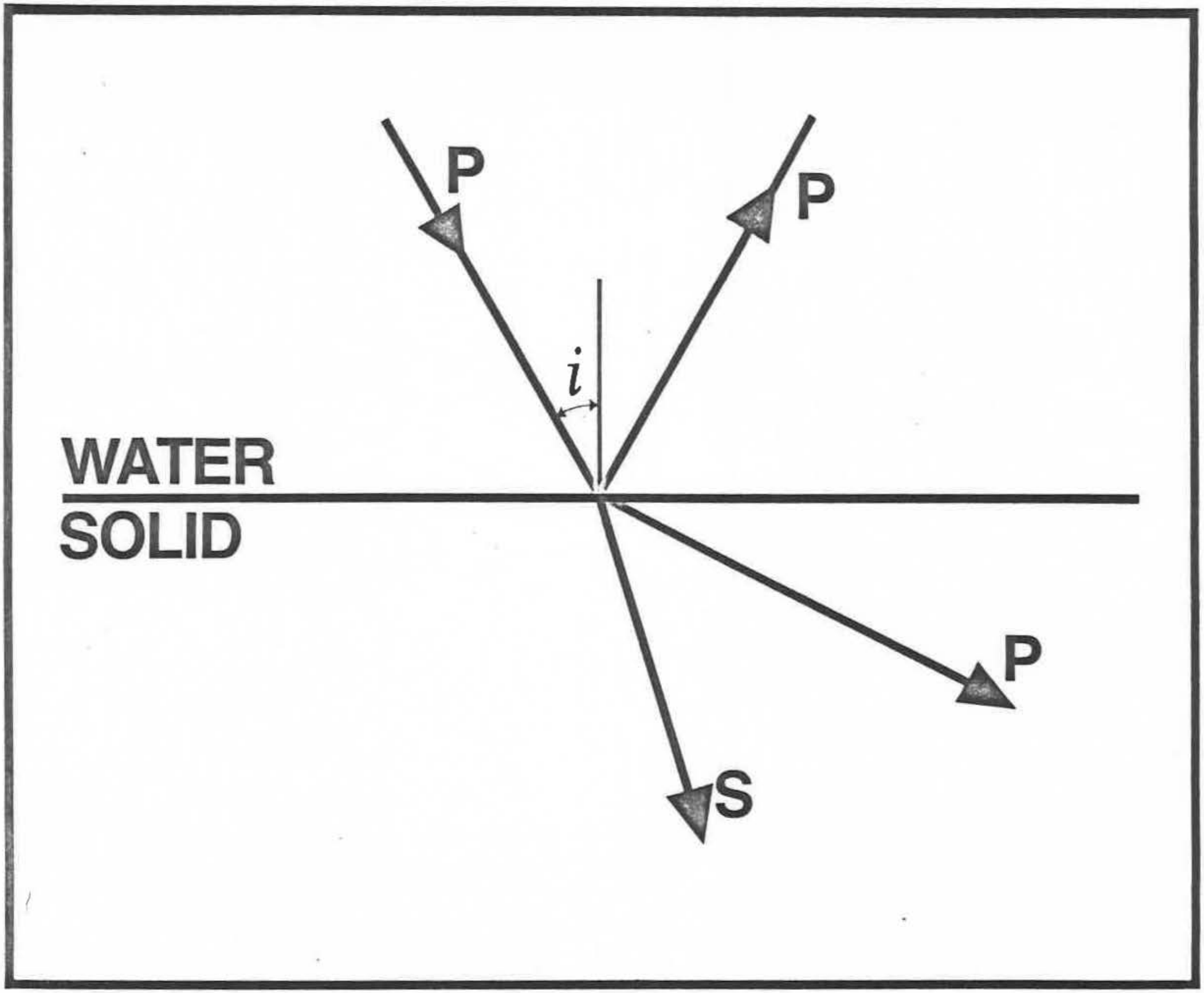

FIGURE 1

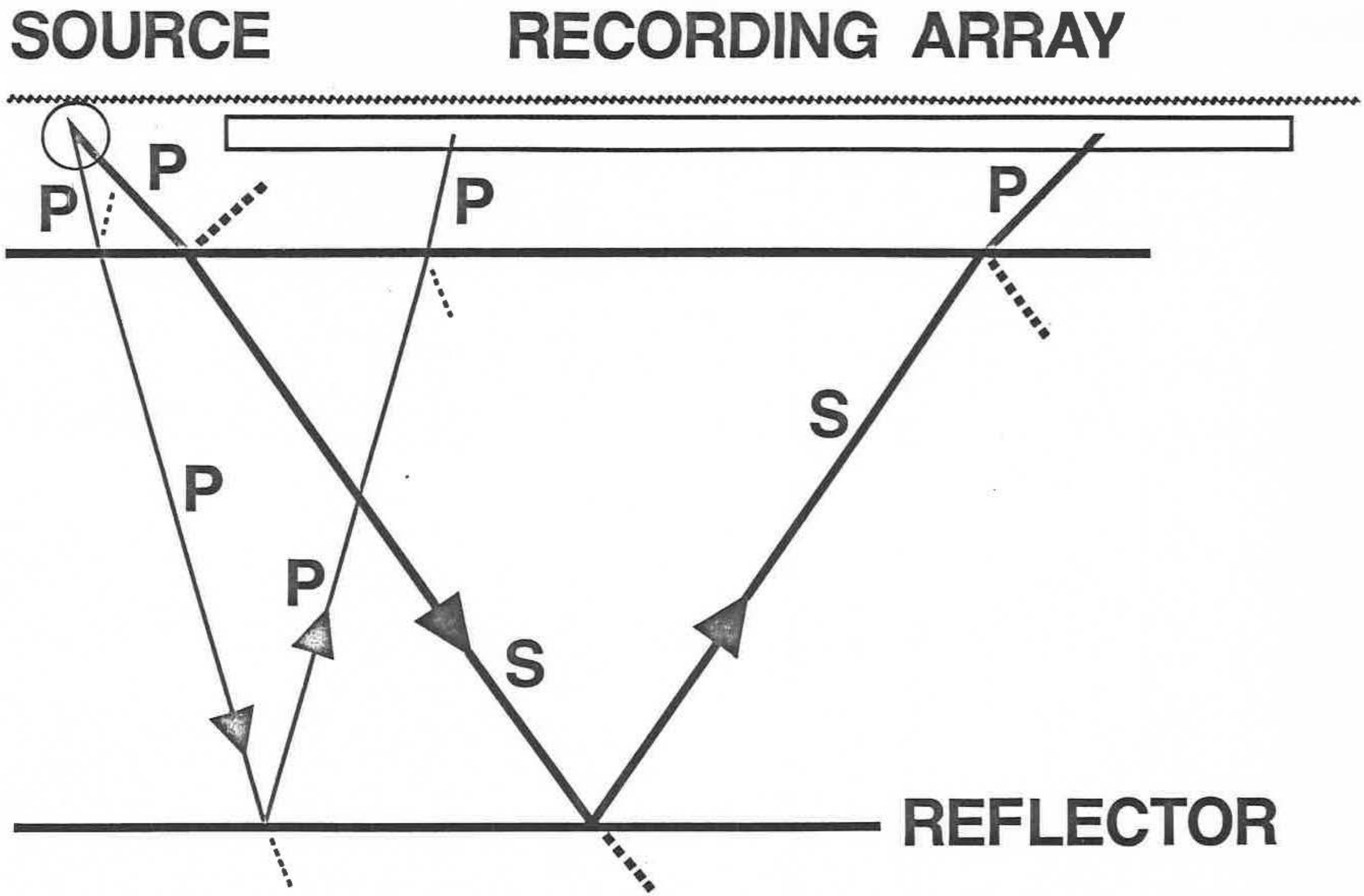

FIGURE 2

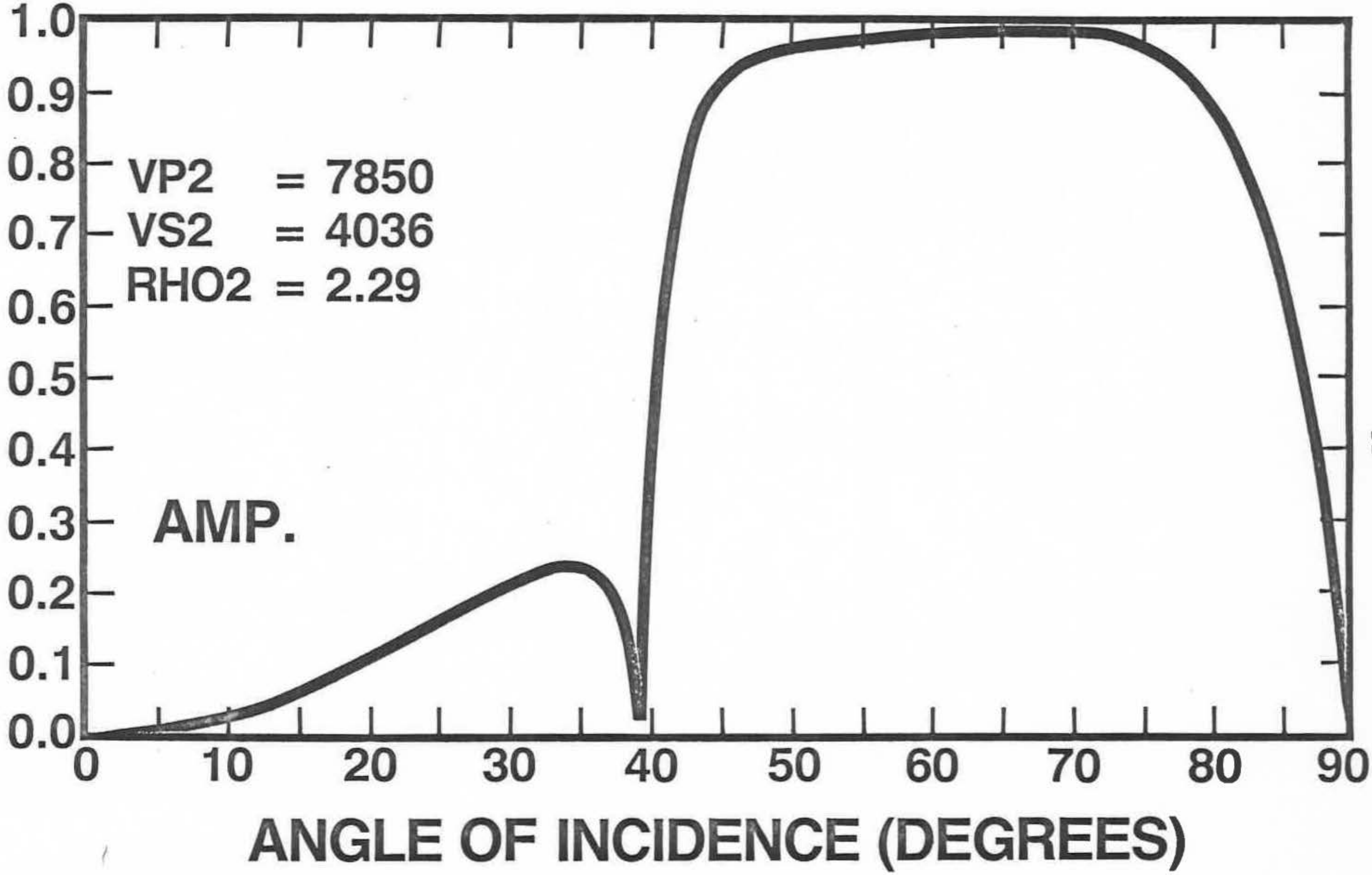
1.0
0.9
0.8
0.7
0.6
0.5
0.4
0.3
0.2
0.1
0.0
VP2 = 7850
VS2 = 4036
RHO2 = 2.29
AMP.
0
10
20
30
40
50
60
70
80
90
ANGLE OF INCIDENCE (DEGREES)

FIGURE 3

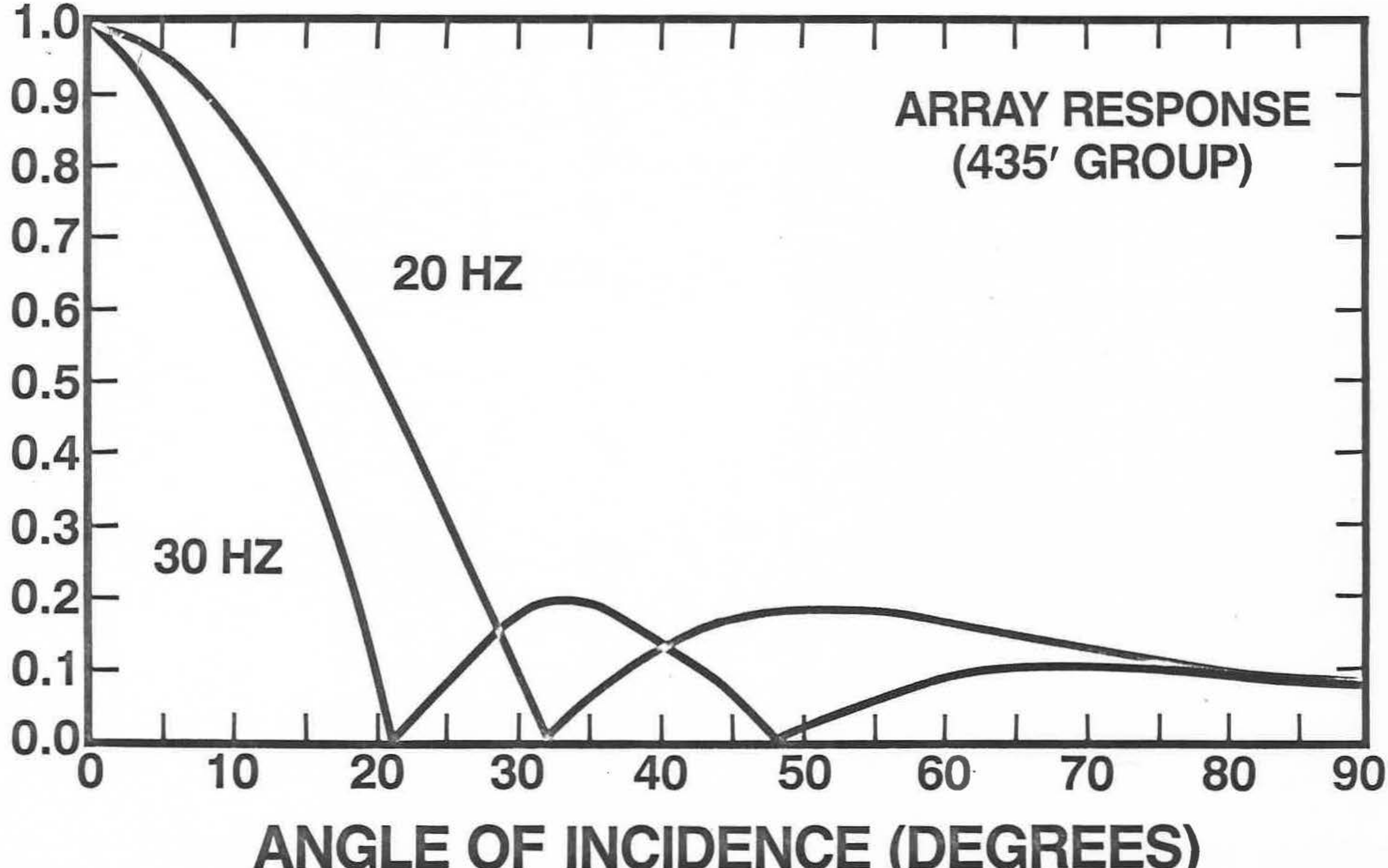

ARRAY RESPONSE
(435′ GROUP)
20 HZ
30 HZ
1.0
0.9
0.8
0.7
0.6
0.5
0.4
0.3
0.2
0.1
0.0
0
10
20
30
40
50
60
70
80
90
ANGLE OF INCIDENCE (DEGREES)

FIGURE 4A

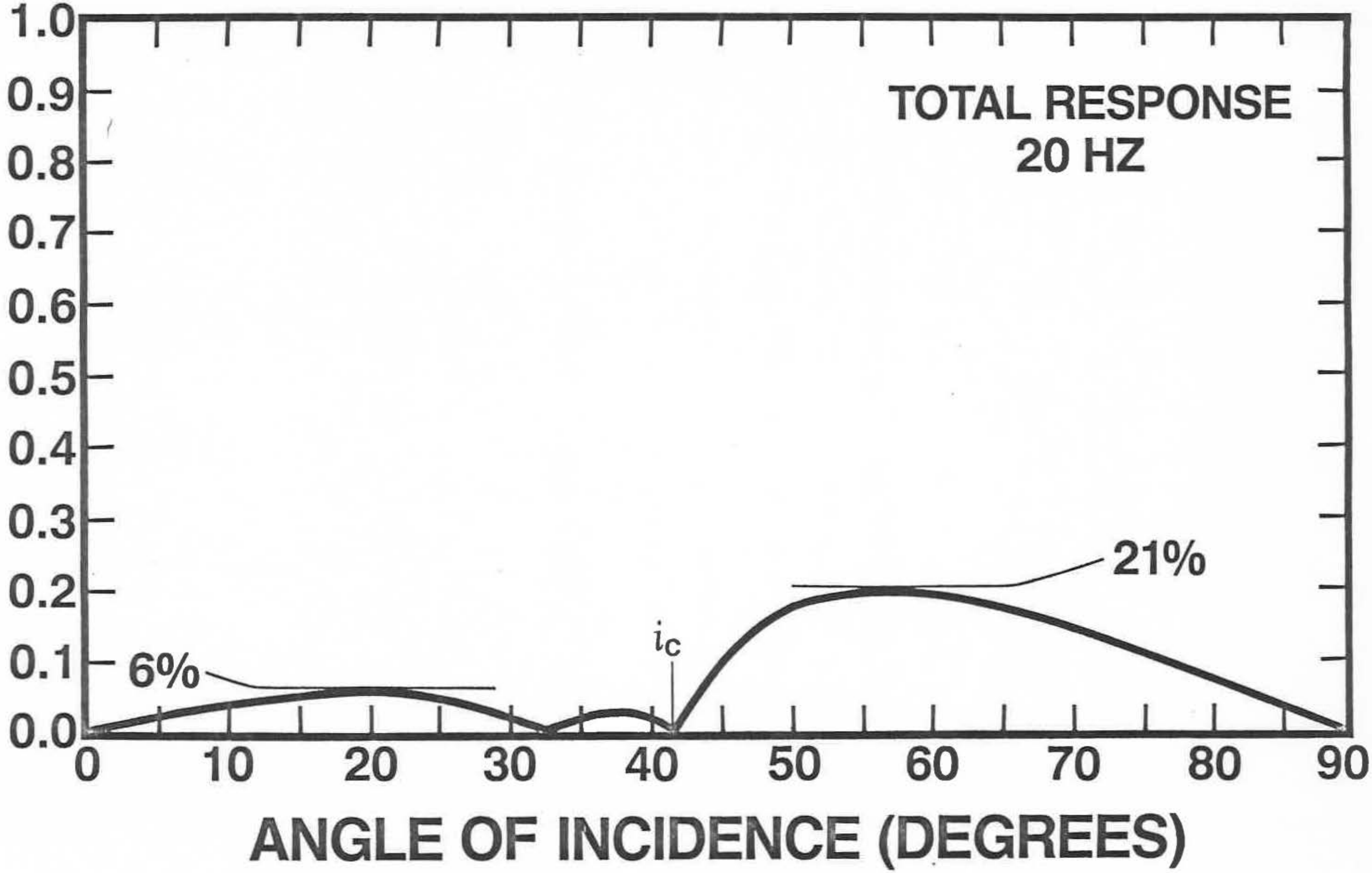
TOTAL RESPONSE
20 HZ
1.0
0.9
0.8
0.7
0.6
0.5
0.4
0.3
0.2
0.1
0.0
6%
21%
i_c
0
10
20
30
40
50
60
70
80
90
ANGLE OF INCIDENCE (DEGREES)

FIGURE 4B

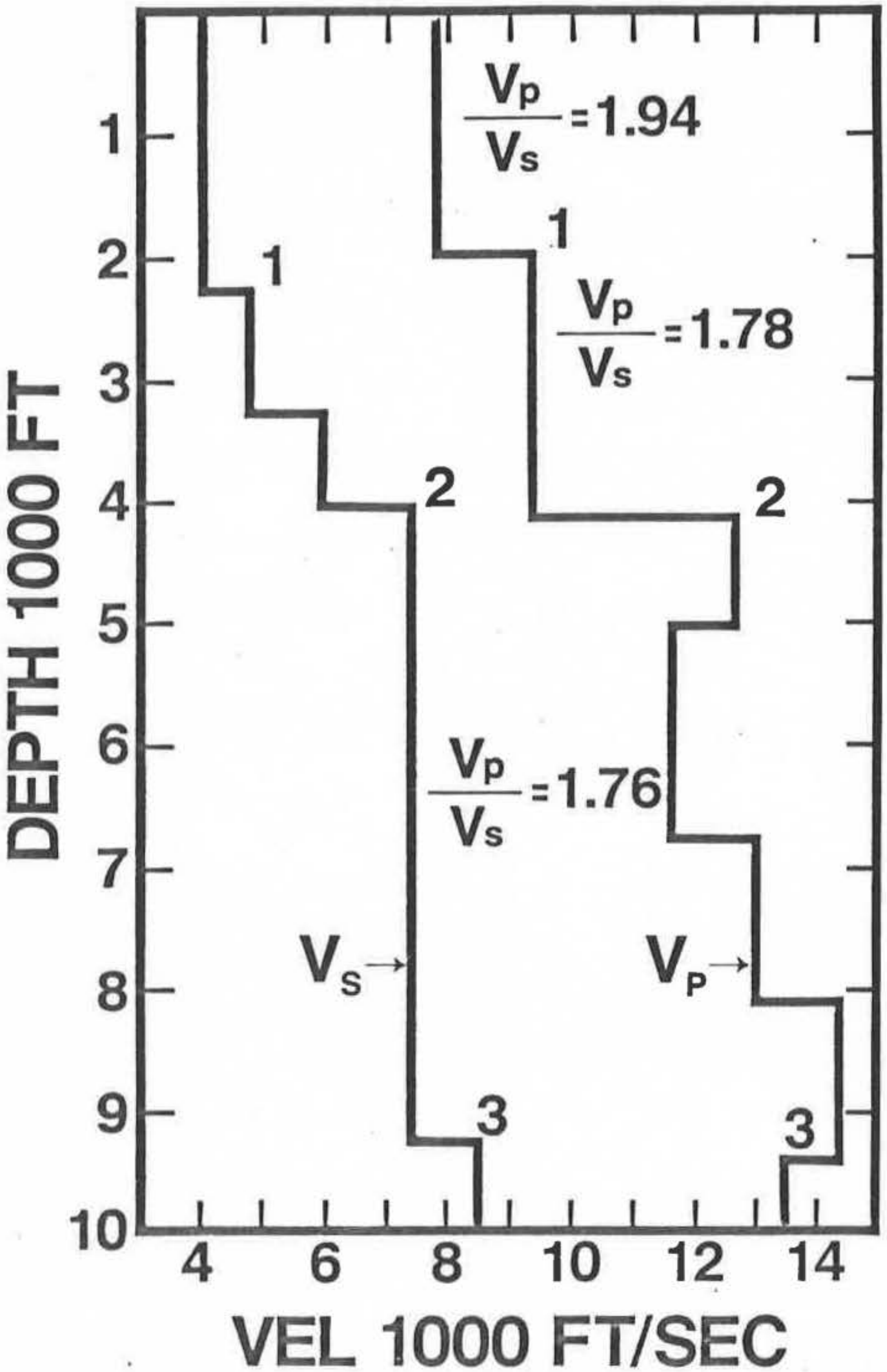

DEPTH 1000 FT
VEL 1000 FT/SEC
1
2
3
4
5
6
7
8
9
10
4
6
8
10
12
14
Vp/Vs = 1.94
Vp/Vs = 1.78
Vp/Vs = 1.76
1
2
3
1
2
3
Vs
Vp

FIGURE 5

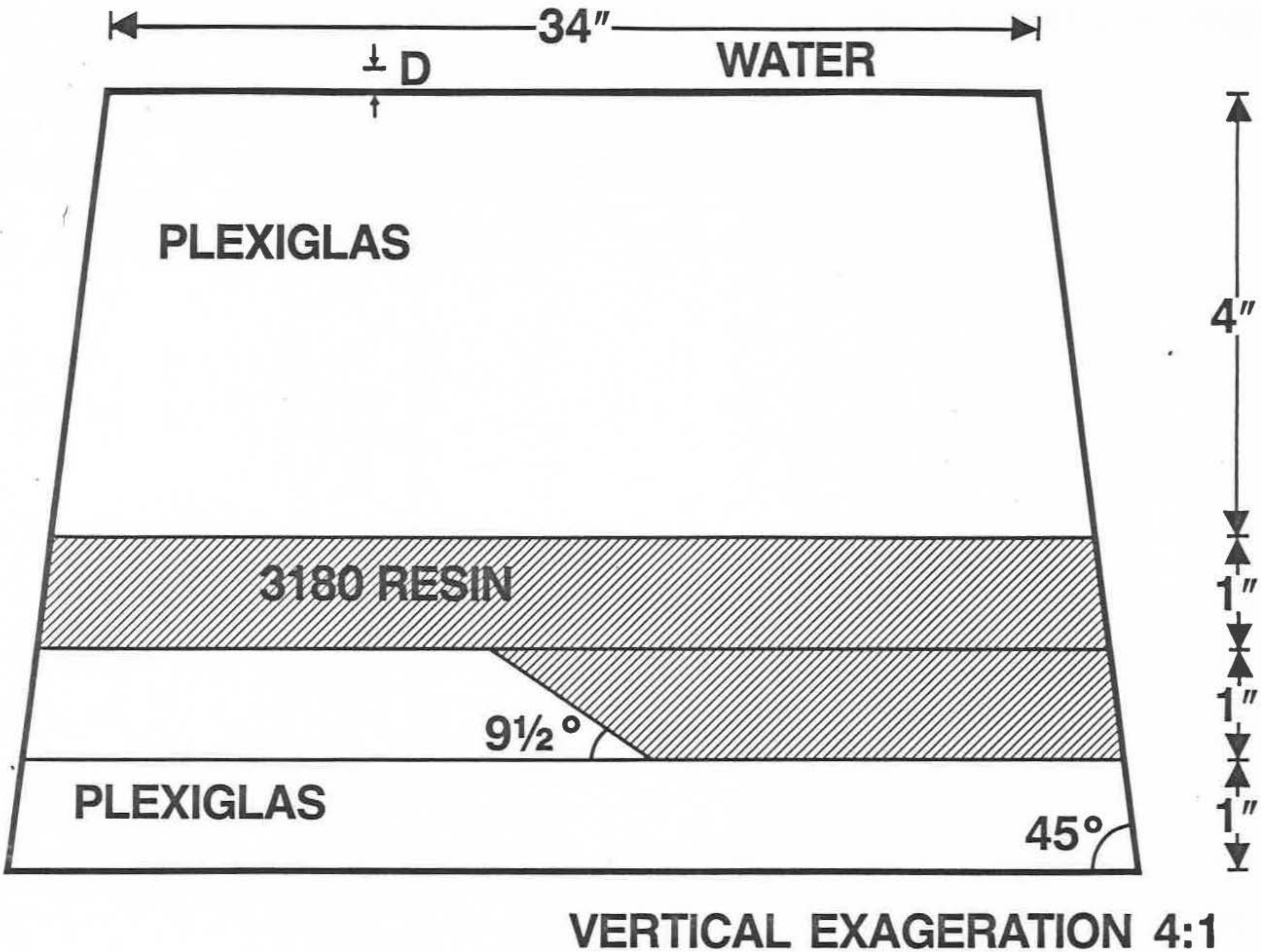
34"
D
WATER
PLEXIGLAS
4"
3180 RESIN
1"
1"
9½°
PLEXIGLAS
45°
1"
VERTICAL EXAGERATION 4:1

FIGURE 6

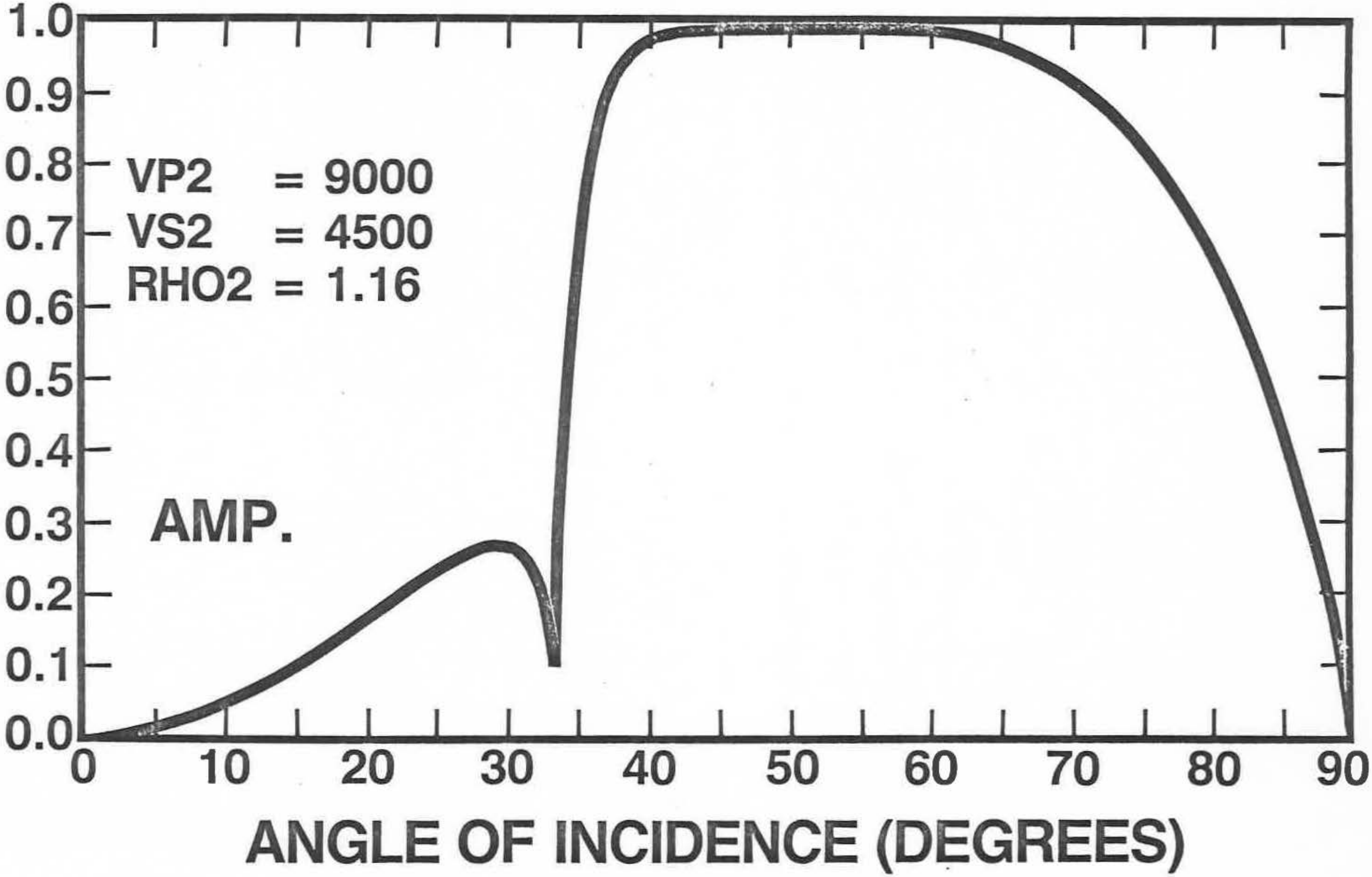
1.0
0.9
0.8
0.7
0.6
0.5
0.4
0.3
0.2
0.1
0.0
VP2 = 9000
VS2 = 4500
RHO2 = 1.16
AMP.
0
10
20
30
40
50
60
70
80
90
ANGLE OF INCIDENCE (DEGREES)

FIGURE 7

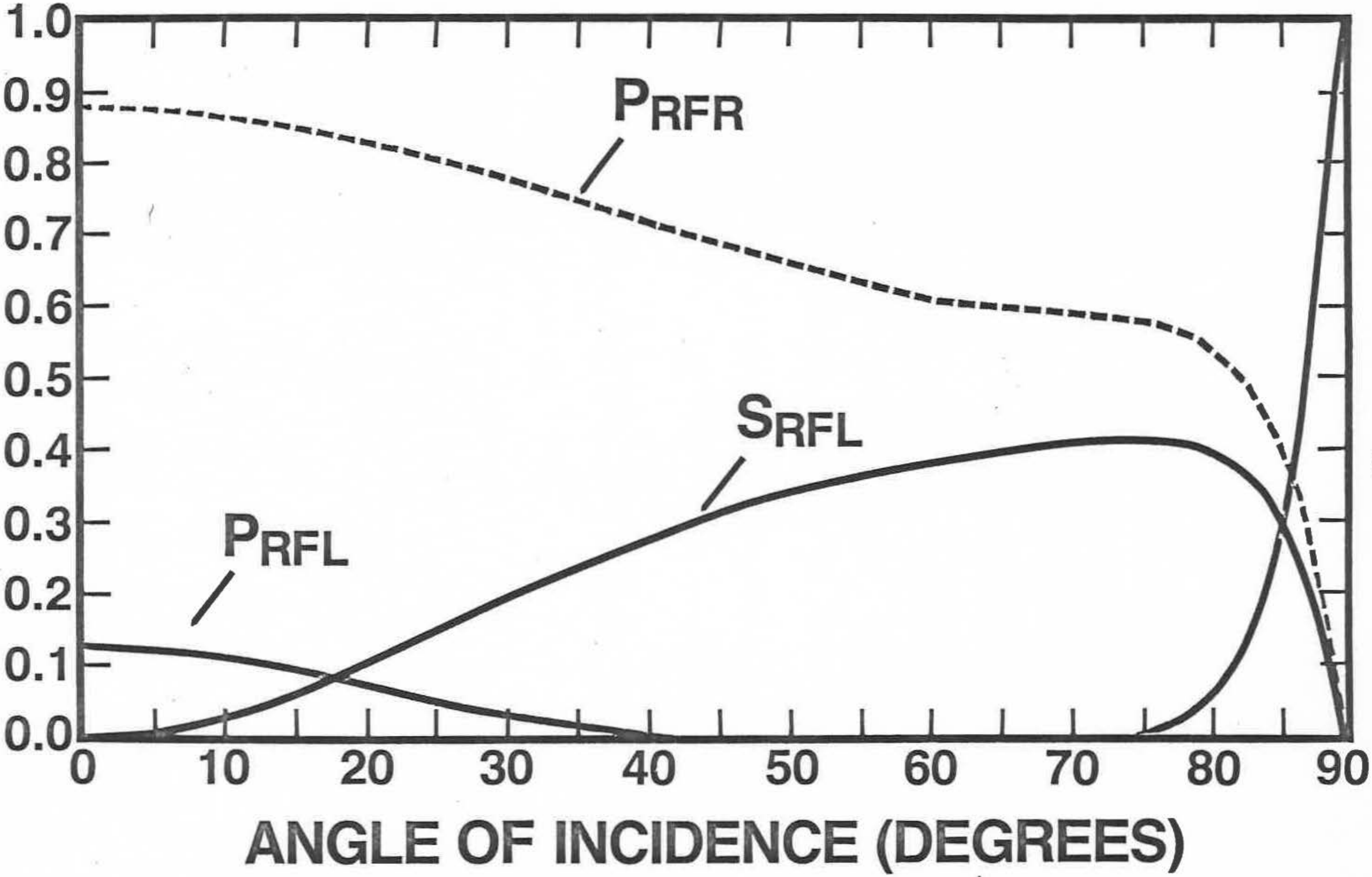

1.0
0.9
0.8
0.7
0.6
0.5
0.4
0.3
0.2
0.1
0.0
PRFR
SRFL
PRFL
0
10
20
30
40
50
60
70
80
90
ANGLE OF INCIDENCE (DEGREES)

FIGURE 8

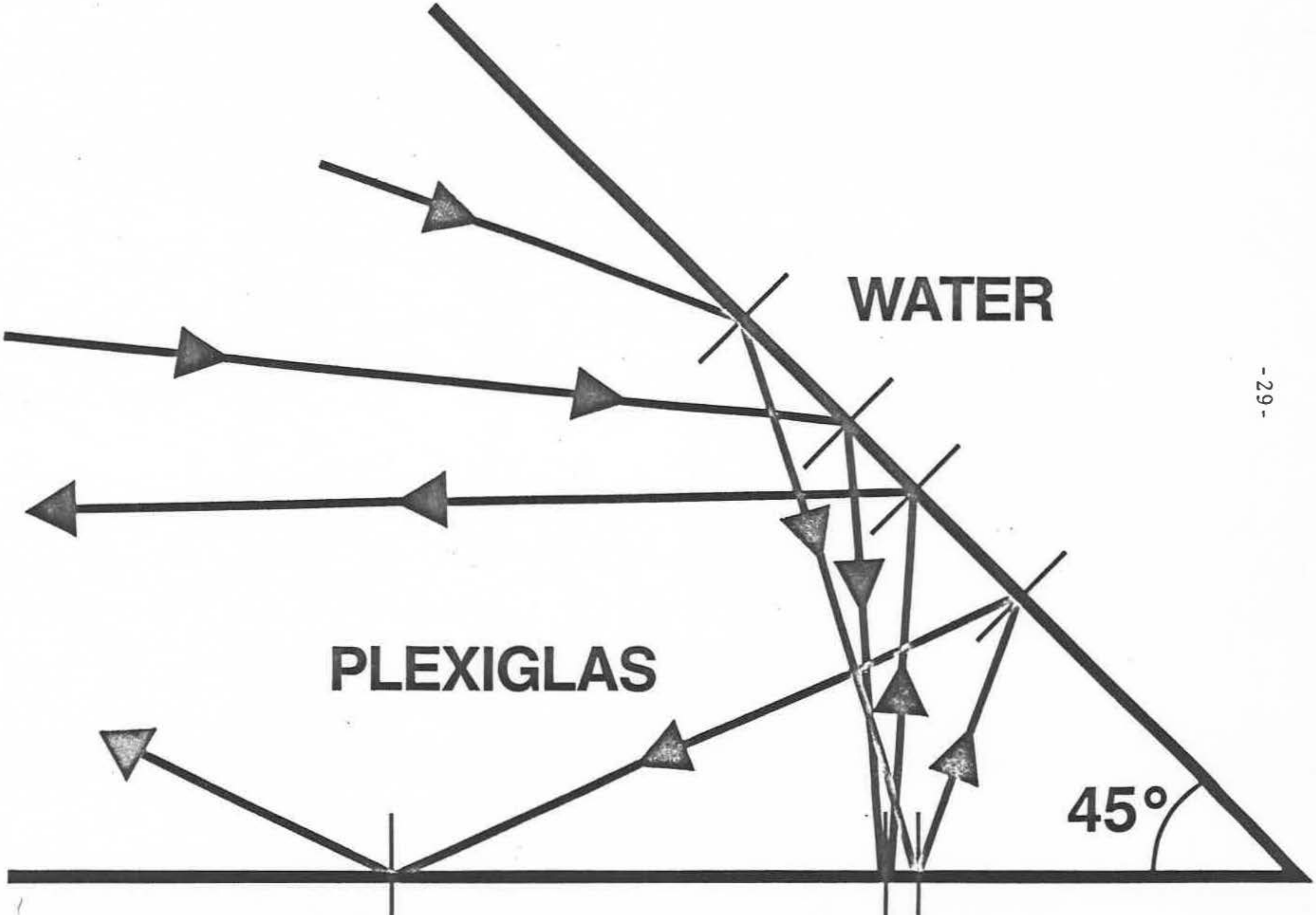

FIGURE 9

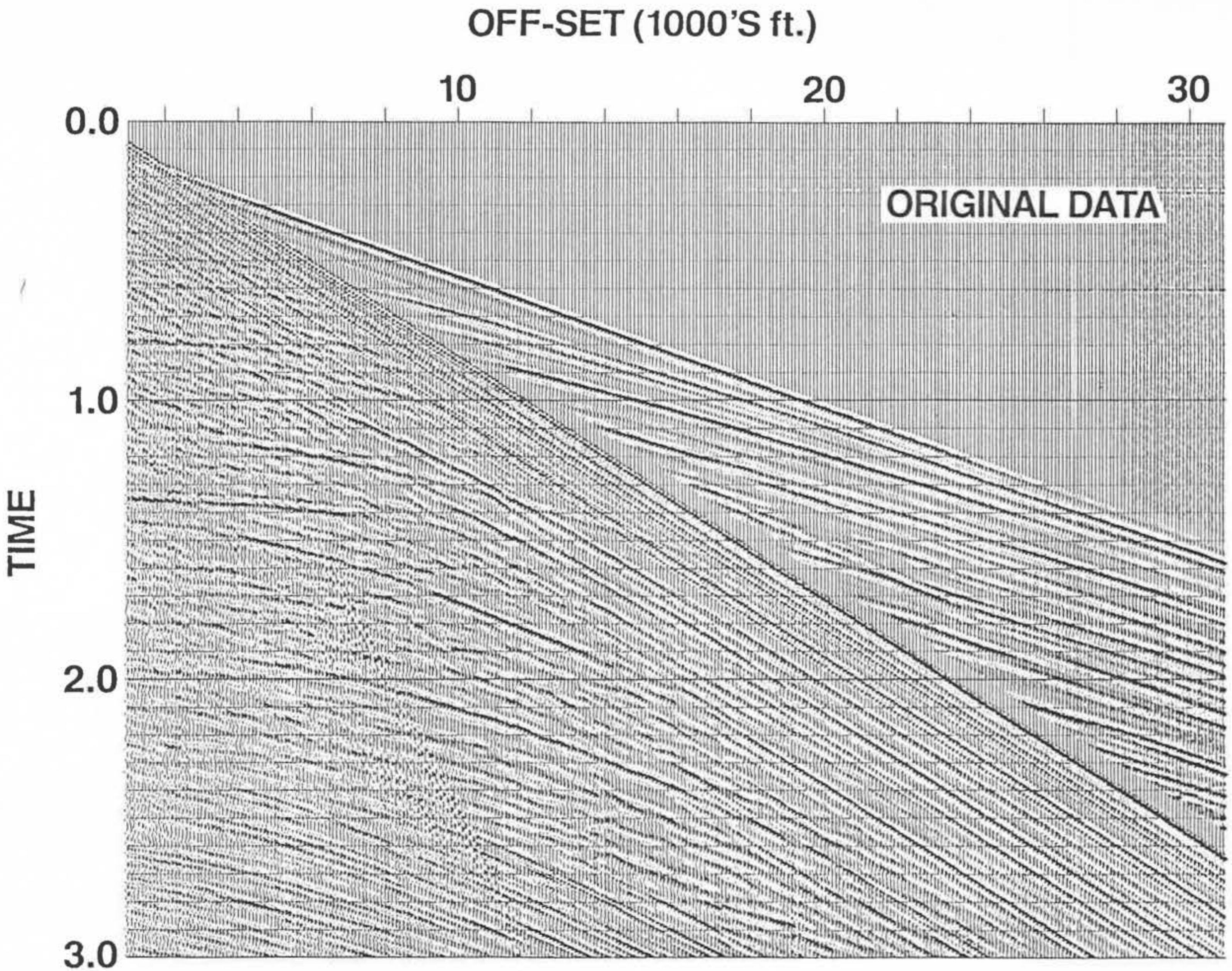

FIGURE 1C

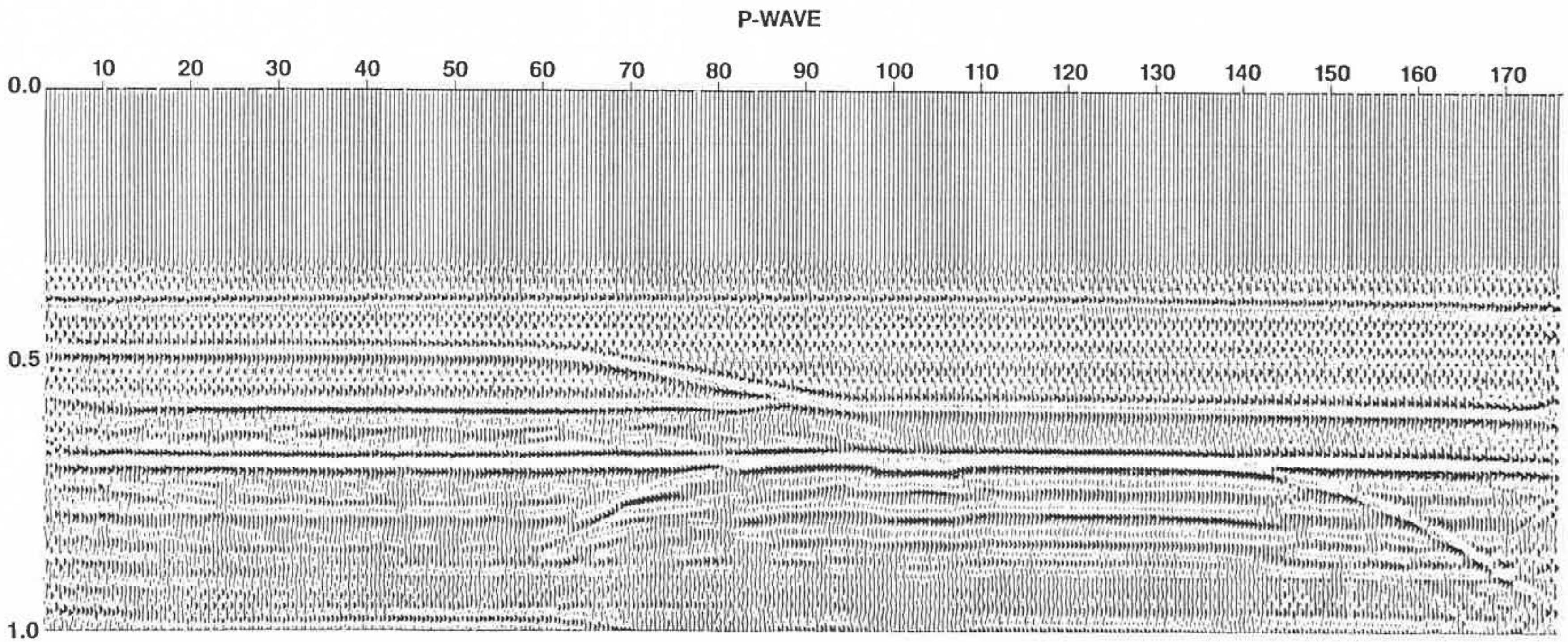
P-WAVE
10
20
30
40
50
60
70
80
90
100
110
120
130
140
150
160
170
0.0
0.5
1.0

FIGURE 11

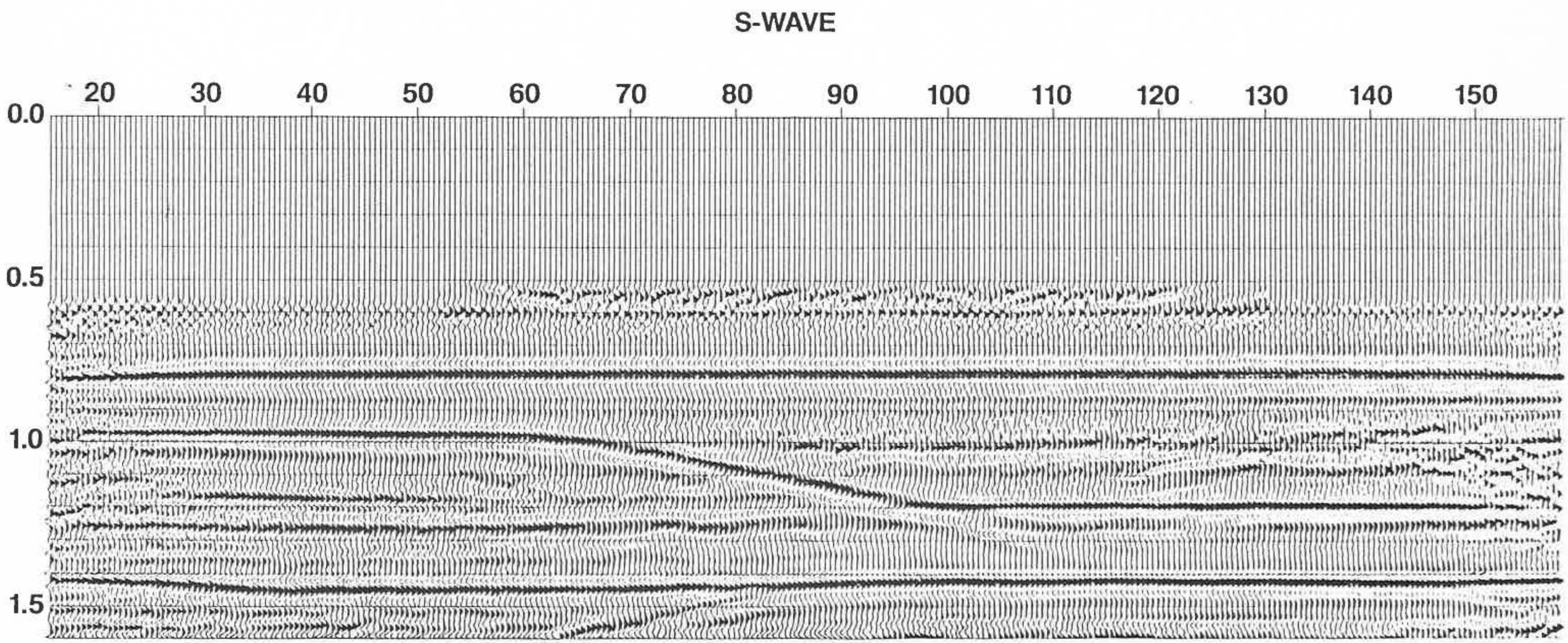

FIGURE 12

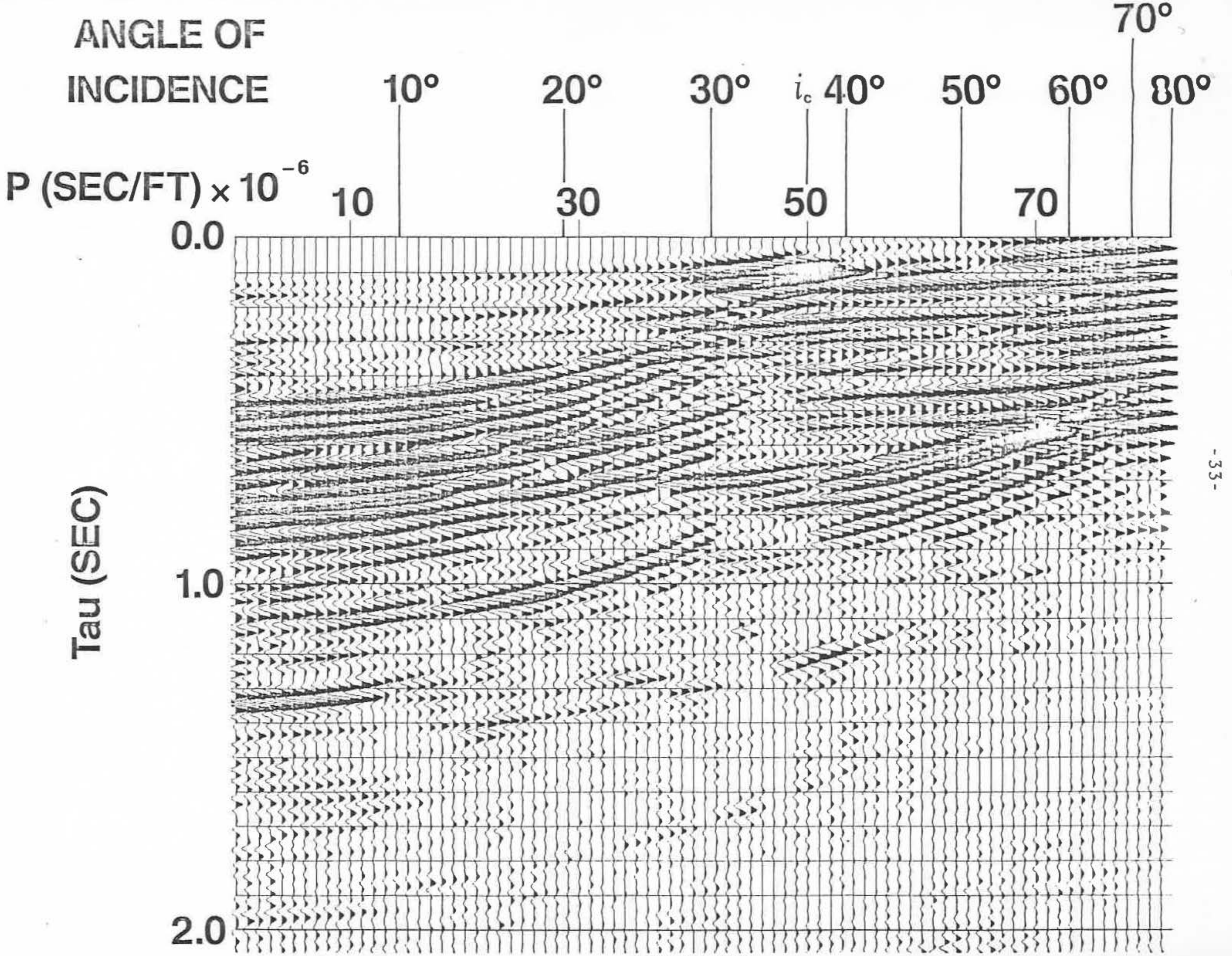
ANGLE OF
INCIDENCE
10°
20°
30°
i_c
40°
50°
60°
70°
80°
P (SEC/FT) × 10^{-6}
10
30
50
70
0.0
1.0
2.0
Tau (SEC)

FIGURE 13A

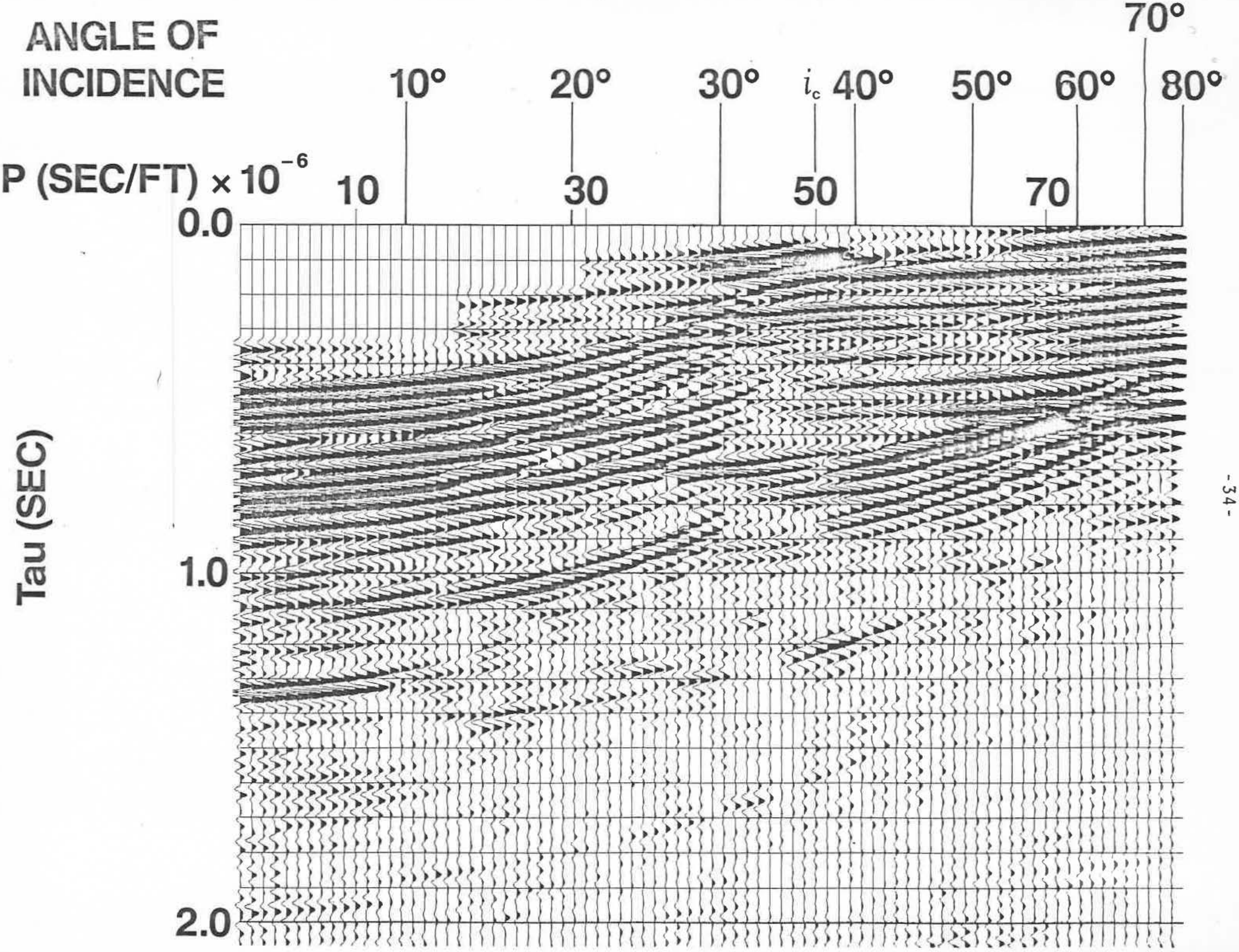
ANGLE OF INCIDENCE
10°
20°
30°
i_c
40°
50°
60°
70°
80°
P (SEC/FT) × 10^{-6}
10
30
50
70
0.0
1.0
2.0
Tau (SEC)

FIGURE 13B

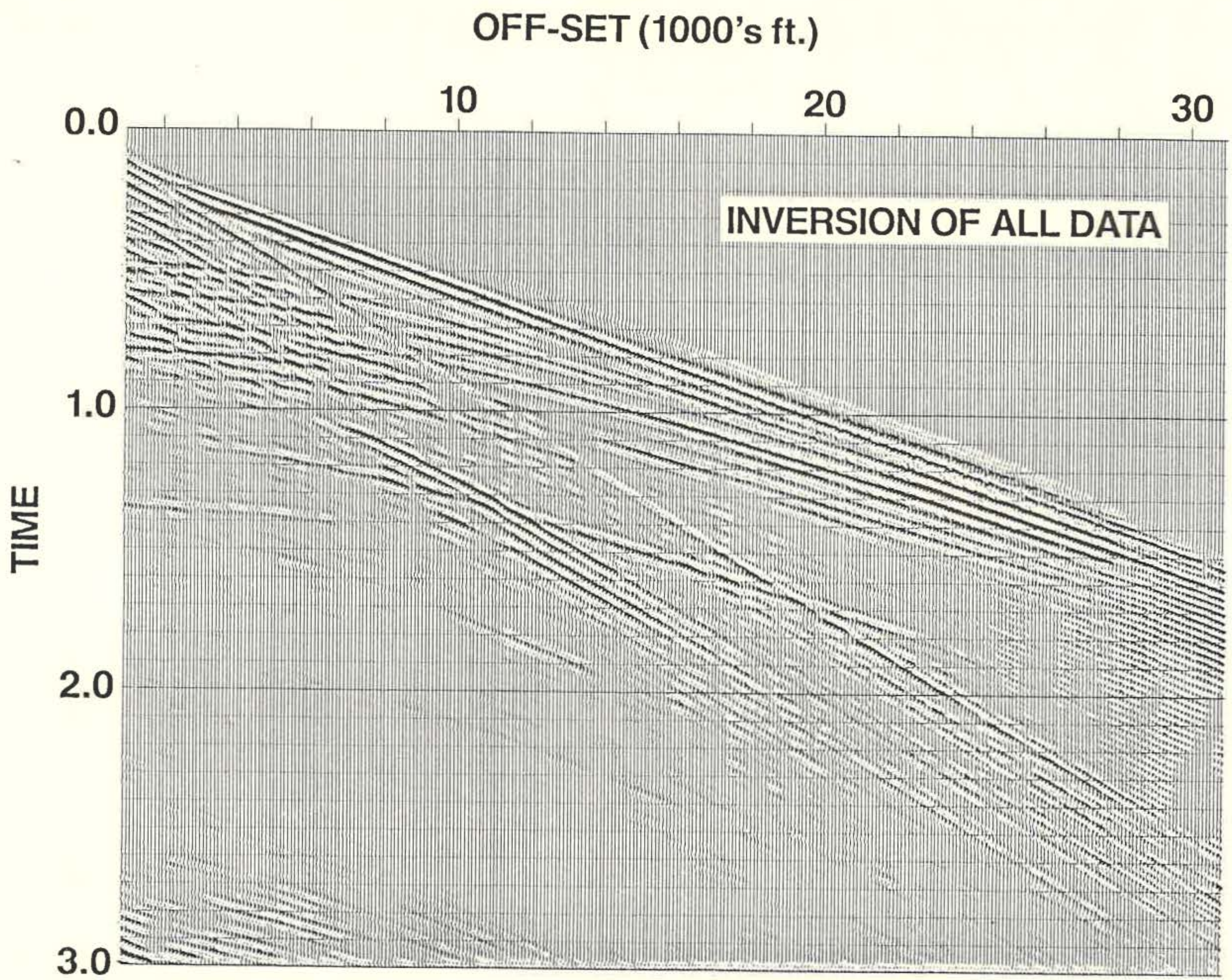

FIGURE 14

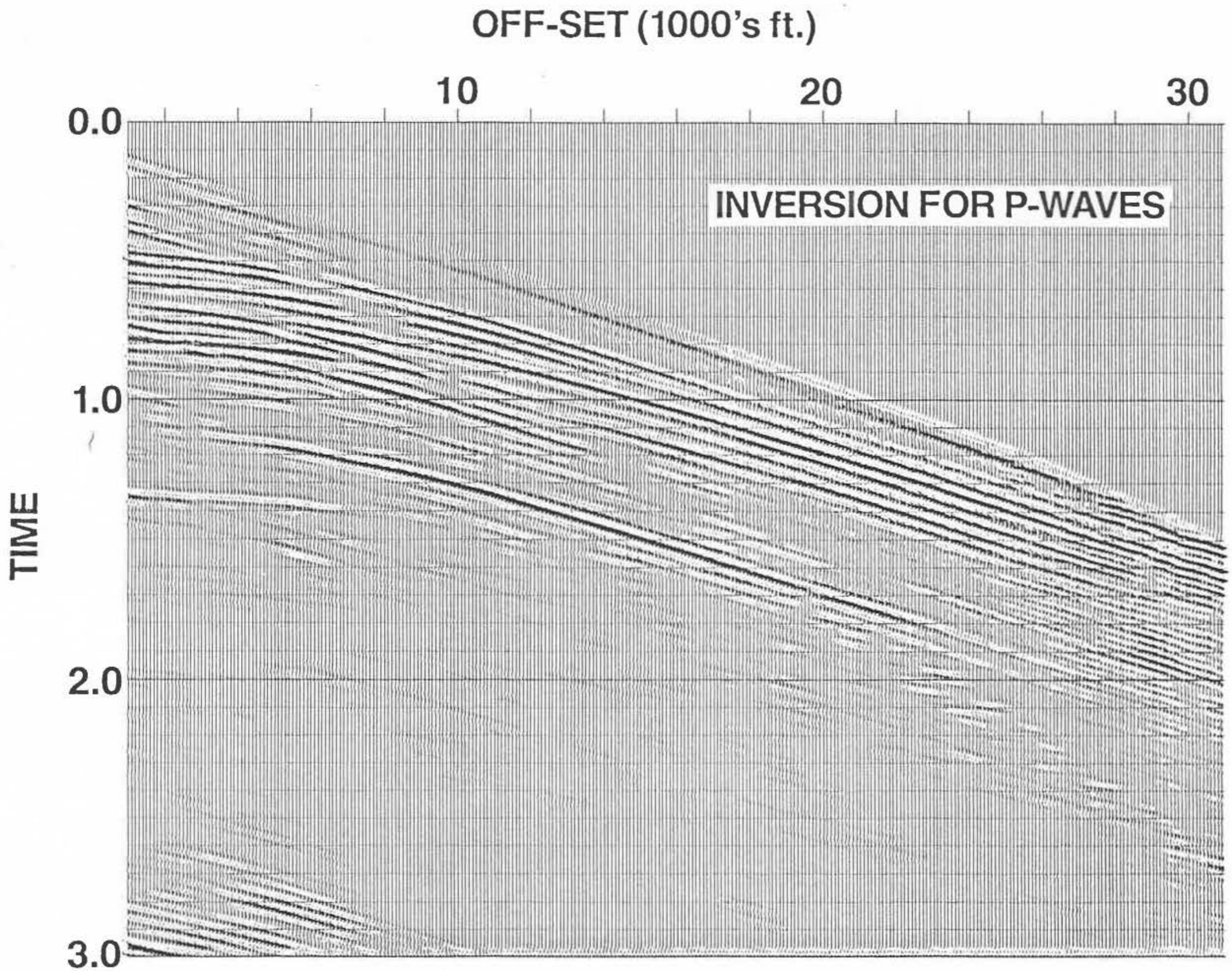

FIGURE 15

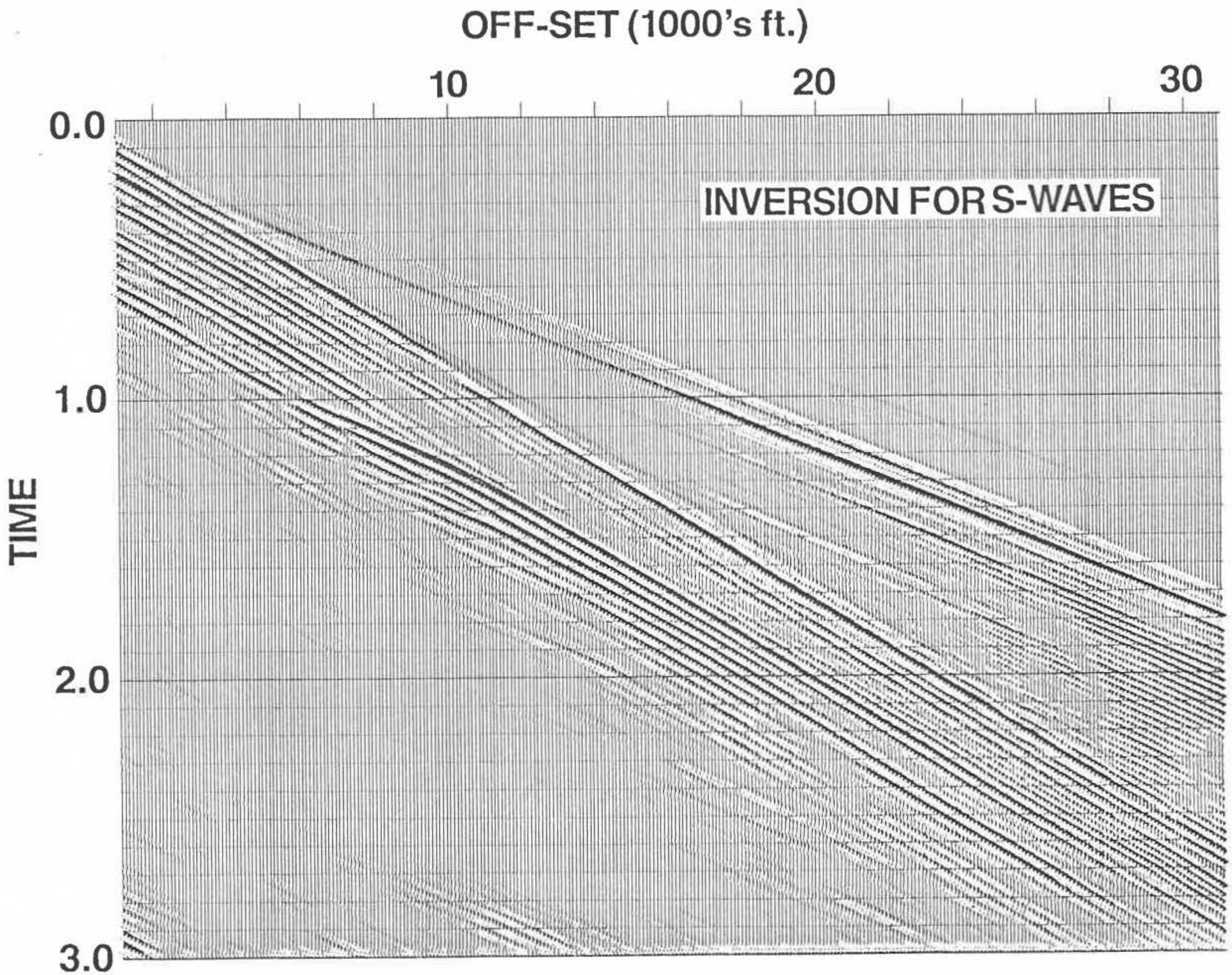

FIGURE 16

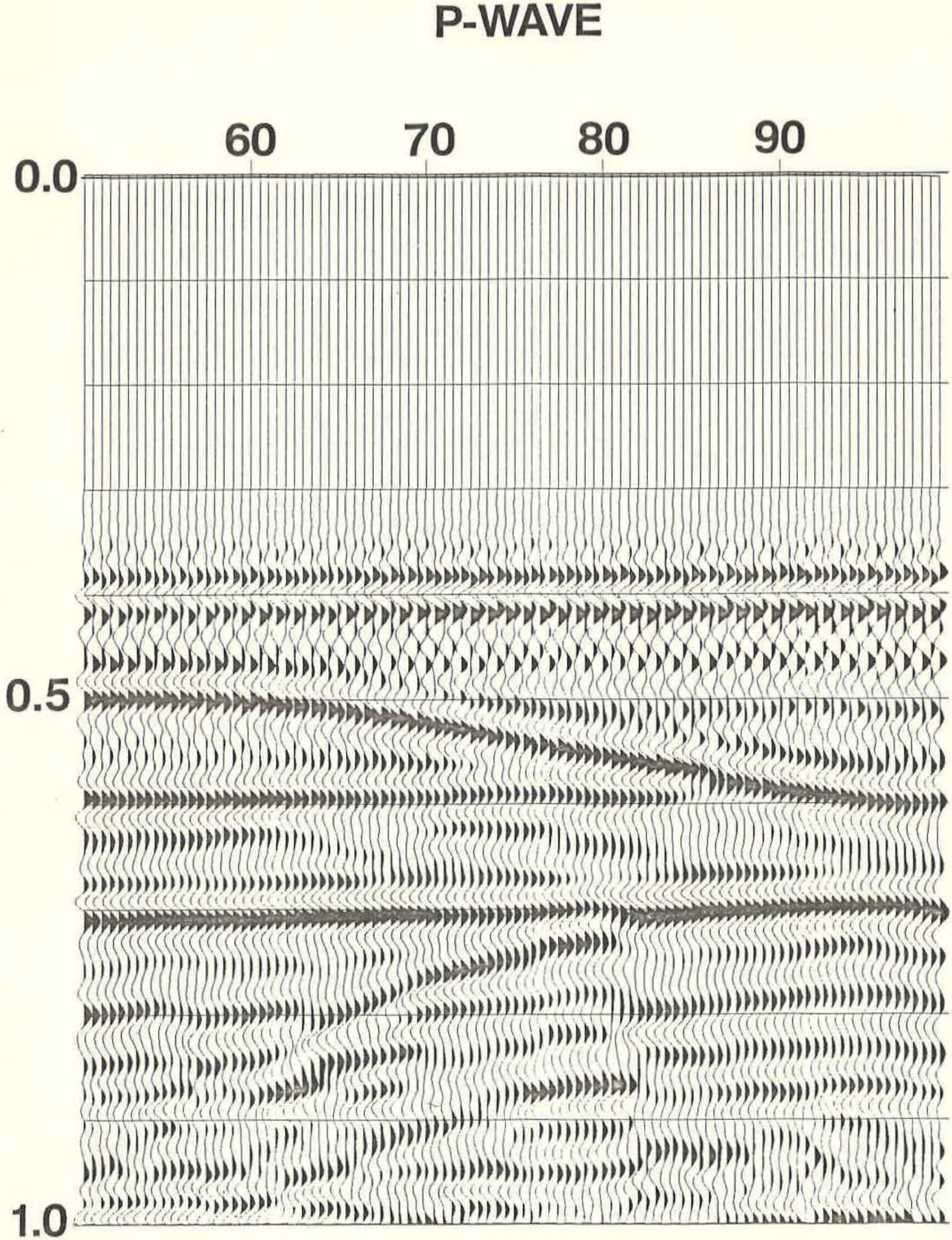

FIGURE 17

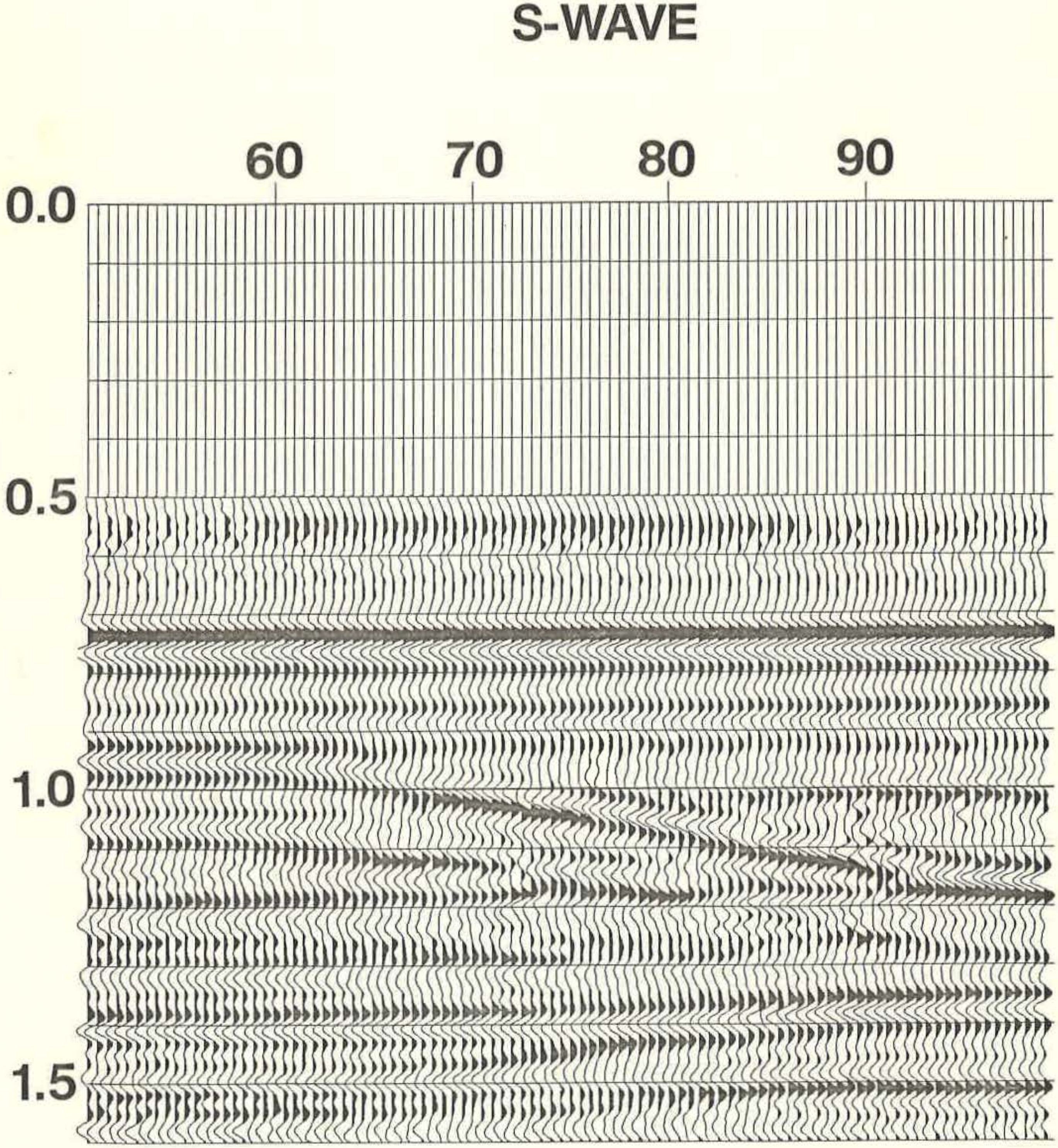

FIGURE 18